ELSEVIER

Biochimica et Biophysica Acta 1464 (2000) 207–218

BIOCHIMICA ET BIOPHYSICA ACTA
BBA

www.elsevier.com/locate/bba

Radiation inactivation studies of hepatic sinusoidal reduced glutathione transport system

Aravind V. Mittur [a], Neil Kaplowitz [a], Ellis S. Kempner [b], Murad Ookhtens [a,*]

[a] *Research Center for Liver Diseases, Department of Medicine, USC School of Medicine, University of Southern California, 2011 Zonal Ave., HMR-615, Los Angeles, CA 90033, USA*

[b] *Laboratory of Physical Biology, NIAMS, National Institutes of Health, Bethesda, MD 20892, USA*

Received 21 October 1999; accepted 11 January 2000

Abstract

Sinusoidal transport of reduced glutathione (GSH) is a carrier-mediated process. Perfused liver and isolated hepatocyte models revealed a low-affinity transporter with sigmoidal kinetics ($K_m \sim 3.2$–12 mM), while studies with sinusoidal membrane vesicles (SMV) revealed a high-affinity unit ($K_m \sim 0.34$ mM) besides a low-affinity one ($K_m \sim 3.5$–7 mM). However, in SMV, both the high- and low-affinity units manifested Michaelis–Menten kinetics of GSH transport. We have now established the sigmoidicity of the low-affinity unit ($K_m \sim 9$) in SMV, consistent with other models, while the high-affinity unit has been retained intact with Michaelis–Menten kinetics ($K_m \sim 0.13$ mM). We capitalized on the negligible cross-contributions of the two units to total transport at the low and high ends of GSH concentrations and investigated their characteristics separately, using radiation inactivation, as we did in canalicular GSH transport (Am. J. Physiol. 274 (1998) G923–G930). We studied the functional sizes of the proteins that mediate high- and low-affinity GSH transport in SMV by inactivation of transport at low (trace and 0.02 mM) and high (25 and 50 mM) concentrations of GSH. The low-affinity unit in SMV was much less affected by radiation than in canalicular membrane vesicles (CMV). The target size of the low-affinity sinusoidal GSH transporter appeared to be considerably smaller than both the canalicular low- and high-affinity transporters. The high-affinity unit in SMV was markedly inactivated upon irradiation, revealing a single protein structure with a functional size of ~70 kDa. This size is indistinguishable from that of the high-affinity GSH transporter in CMV reported earlier.

Keywords: Glutathione transport; Target size analysis; Sinusoidal membrane vesicle

1. Introduction

Reduced glutathione (GSH), an endogenous antioxidant, is exported from hepatocytes across basolateral (sinusoidal) and apical plasma membrane domains, with both components of efflux manifesting maturational changes [1]. Sinusoidal efflux serves as the principal source of plasma GSH, cysteine and cystine [2–5]. The latter two arise from extracellular hydrolysis of plasma GSH (by the ecto-enzyme γ-

Abbreviations: GSH, reduced glutathione; *n*, number of binding/transport sites for a substrate in a transport system; SMV, sinusoidal membrane vesicles; CMV, canalicular membrane vesicles; DTT, dithiothreitol; BSP-SG, sulfobromophthalein–glutathione conjugate; HPLC, high-performance liquid chromatography; oatp1, organic anion transporter polypeptide 1

* Corresponding author. Fax: +1-323-442-3250;
E-mail: murad@hsc.usc.edu

0005-2736/00/$ – see front matter
PII: S0005-2736(00)00152-8

glutamyl-transpeptidase) to cysteine, which is subsequently oxidized to cystine. Using tracer-kinetic methods in vivo and multicompartmental analysis and modeling, we have defined the kinetics of plasma GSH, cysteine and cystine turnover and shown that, in mature, ad libitum-fed rats, essentially all of plasma cysteine and cystine are derived from plasma GSH [4,5]. Thus, sinusoidal GSH efflux plays a critical role in the inter-organ homeostasis of GSH and thiol-disulfides and regulation of the redox status of plasma. Since certain disulfides (cystine) and thiol-reducing agents (DTT) have been shown to modulate hepatic sinusoidal GSH transport [6,7], it is possible that sinusoidal GSH efflux may be modulated by the redox status of hepatic cytosol and/or blood plasma. Such modulatory effects, mediated by the redox status of intra- and extrahepatic environment, could serve as critical determinants of changes in GSH homeostasis during sustained oxidative injury as well as aging [8,9].

Using a variety of experimental models ranging from isolated perfused livers [10] to freshly isolated and/or cultured hepatocytes [6,7,11,12], to SMV [13,14], sinusoidal GSH transport has been found to be saturable and inhibitable by various amino acids and organic anions in unconjugated and conjugated forms. These include *trans*-inhibition by methionine and cystathionine [15–17] and *cis*-inhibition by bilirubin (in unconjugated and mono- and di-glucuronide forms) and BSP-SG [10,17–19]. These findings have indicated the involvement of carrier proteins in sinusoidal transport of GSH which remain to be directly identified since a putative sinusoidal transporter clone [20] proved to represent an *Escherichia coli* cloning artifact (Kaplowitz et al., unpublished observations).

It is known that organic anion transporter polypeptide 1 (oatp1) may mediate the transport of glutathione, possibly in exchange with taurocholate [21]. However, the transport of taurocholate by oatp1 was neither modulated by DTT nor inhibited by methionine and cystathionine [21]. Furthermore, the transport of substrates by oatp1 is expected to be an electroneutral process, whereas efflux of GSH with sinusoidal characteristics in a number of models is electrogenic [6,7,11–14]. Therefore, the contribution of oatp1 to GSH transport in hepatocytes is not clear and is presumed to be minimal. Thus, it is plausible that other candidate proteins may exist as the principal transporter(s) of hepatic sinusoidal GSH.

Heretofore, perfused liver, freshly isolated and cultured hepatocyte models have consistently and unequivocally revealed the presence of a low-affinity transport unit that displays non-Michaelis–Menten, i.e., sigmoidal kinetics ($K_m \sim 3.2$–12 mM; Hill coefficient $n \sim 2$–3). On the other hand, studies with SMV succeeded in identifying an additional, high-affinity unit with Michaelis–Menten kinetics ($K_m \sim 0.34$ mM) [14]. This high-affinity unit was not revealed in studies of sinusoidal GSH efflux in the perfused liver and isolated cell models, in all likelihood due to the difficulty of measurement and scatter of the intra- and extracellular GSH data at diminishing cellular GSH concentrations. However, while both the high- and low-affinity units were revealed in earlier SMV studies [13,14], the low affinity unit ($K_m \sim 3.5$–7 mM) failed to manifest sigmoidal kinetics of transport.

In pilot studies, attempting to refine and improve our membrane fractionation and transport measurement techniques, we were able for the first time to reveal the sigmoidicity in the kinetics of GSH transport by the low-affinity unit in SMV, while the high-affinity, Michaelis–Menten unit was retained. This outcome prompted us to design the present study with the following purposes in mind: (1) define the kinetics of GSH transport in SMV and determine the kinetic parameters of the high- and low-affinity units to assess the cross-contributions to total transport by the two units; (2) If cross-contributions are negligible at the low and high ends of GSH concentrations, use radiation inactivation of GSH transport in SMV to study the characteristics of each transporter individually, as we did earlier in GSH transport in CMV [22].

Radiation inactivation is a unique and powerful tool that allows the estimation of the functional size of proteins in situ [23,24]. It can be applied to detect the presence of multiple proteins with distinct sizes, which may share common functions. As stated above, although oatp1 has been identified as a candidate GSH transporter, it cannot account for all of the observed functional and kinetic features of hepatic sinusoidal GSH transport. In all likelihood, other protein(s) that mediate GSH transport remain to be identified. Radiation inactivation can reveal the

presence of multiple GSH transporters, if their functional sizes are distinct, and thus enable us to compare their sizes with oatp1. Furthermore, functional interaction of the transporter(s) with other distinct proteins can also be tested using target size analysis.

We have earlier applied the radiation inactivation technique to successfully identify and study the properties of the high- and low-affinity GSH transporters in canalicular membrane vesicles (CMV) [22]. In our SMV model, the presence of a high-affinity Michaelis–Menten unit suggests the involvement of a protein distinct from the low-affinity carrier. The sigmoidal kinetics of the low-affinity transport could indicate positive cooperativity between subunits in an oligomeric carrier or between multiple sites on a single polypeptide. Thus, knowledge of the in situ functional size of hepatic sinusoidal GSH transport could potentially help to clarify the structural basis of the two affinities for GSH and the sigmoidicity in the low-affinity transport.

Our studies were designed to answer the following questions. (1) Does the low affinity unit of GSH transport exhibit sigmoidal kinetics with characteristics that result in negligible cross-contribution to total transport by the high- and low-affinity units at the low and high ends of GSH concentrations? (2) If so, are the functional sizes of the high- and low-affinity units of GSH transport, as determined by radiation inactivation, distinct from each other? (3) Is the sigmoidicity of the kinetics of GSH transport by the low-affinity unit due to an oligomeric association of subunits? (4) What are the comparisons among the functional sizes of the sinusoidal high- and low-affinity transporters of GSH with those of the canalicular GSH transporters and oatp1?

2. Materials and methods

2.1. Chemicals and assays

All chemicals were purchased from Sigma Chemical Co. (St. Louis, MO) or other commercial sources. [^{35}S]GSH (>100 Ci/mmol), [^{3}H]GSH (>100 Ci/mmol), [^{3}H]alanine (>75 Ci/mmol), [^{3}H]taurocholic acid (>2 Ci/mmol), L-[^{3}H]glutamate (>40 Ci/mmol), and Aquasol scintillation cocktail were procured from New England Nuclear (Boston, MA). The purity and chemical form of every lot of [^{35}S]GSH was confirmed by radio-HPLC [22,25]. 5′-Nucleotidase was assayed by HPLC [26]. All other assays were performed as described before [22]. BSP-SG was synthesized by the conjugation of BSP and GSH [27]. The resulting product was further purified by size-exclusion chromatography on a Sephacryl S-200 (Pharmacia Biotech) column (2 l bed volume). BSP-SG and GSH were sequentially eluted with deionized water. Fractions with BSP-SG were identified by alkalizing with 1 N NaOH, followed by measuring absorbance at 580 nm. The fractions containing BSP-SG were pooled, lyophilized, and stored at −80°C. BSP-SG was essentially free of GSH and BSP, as verified by HPLC [28].

2.2. Animals

Mature (90–135-day-old), male Sprague–Dawley rats weighing 380–450 g (Harlan Laboratories, San Diego, CA), were housed in a constant temperature and humidity environment, with alternating 12-h light and dark cycles. The rats had access to water and Purina Rodent Chow ad libitum.

2.3. Isolation and characterization of membrane vesicles

We prepared SMV essentially by the method of Meier et al. [29] with certain modifications, which included an added step of initially passing the liver tissue through a stainless-steel sieve (No. 18) (VWR Scientific) to eliminate connective tissue as best possible, before homogenization. The SMV were suspended in cryoprotective buffer with 14% (v/v) glycerol, 1.4% D-sorbitol (w/v), 150 mM KCl, 0.2 mM $CaCl_2$, 0.2 mM $MgCl_2$, and 10 mM Hepes/Tris (pH 7.5). The purity and enrichment of membrane fractions were determined by marker enzymes as described before [22,30]. Storage and handling of the isolated vesicles were performed exactly as described before [22].

2.4. Radiation inactivation and target size analyses

SMV were irradiated exactly as described in an earlier study with CMV [22]. Radiation dosimetry

and sample handling were performed as described before [22,31]. The inactivation of 5′-nucleotidase was again used as an internal control to monitor and establish the dosimetry and consistency of irradiations in individual vesicle preparations [22,32]. Post-irradiation residual transport activity (V) was normalized to transport activity in the unirradiated control (V_o) and expressed as $\%V/V_o$. The semi-log slope of the inactivation curve (ln V/V_o against radiation dose, D) was estimated by fitting the data from both individual experiments and by fitting the mean of residual activities in each group. In cases where a radiation-insensitive component of activity was present, the data were analyzed by the inclusion of a constant in addition to exponentials, as described before [22,33]. The functional size M (in Da) was estimated from the rate constant (μ) of the exponential defining the inactivation curve using the relationship, $M = -17.9 \times 10^5\ \mu$, as described [31].

2.5. Transport studies

The details of our techniques to measure the initial rates of transport of radiolabeled substrates using the rapid filtration technique have been described earlier [22]. We have reduced the time point used to estimate the initial rates of uptake to 10 s from 15 s, used in earlier studies [13,30], to ensure staying within the linear range of uptake at all concentrations of the substrates. In each preparation and at all substrate concentrations, the measurements were made in duplicate and the mean values of the duplicate determinations were used. The duplicates were reproducible, indicating the precision of the techniques applied. The Na^+-dependent transport of [^{3}H]alanine was determined as described [34]. The uptake of GSH under voltage-clamped conditions was determined as described before [13,22]. Aliquots of unirradiated control SMV were handled and processed in the same way as the irradiated ones. The uptake of GSH in the irradiated SMV was measured in parallel and compared to the uptake in corresponding unirradiated controls. *trans*-Stimulation of 2 mM GSH uptake was determined in SMV that were pre-loaded with 10 mM GSH by incubating for 30 min at 25°C. Control SMV were pre-incubated identically, but without GSH.

2.6. Separation of the high- and low-affinity components of GSH transport

We estimated the functional sizes of the two kinetic components by inactivating GSH transport at concentrations where one of the kinetic components was predominant. At 0.02 μM (trace) and 0.02 mM GSH, the high-affinity component was the dominant ($>99.9\%$) transporter, while at 25 and 50 mM GSH, $\geq 95\%$ of total transport was mediated by the low-affinity component (see below and Fig. 2).

2.7. Kinetic analysis and fitting of transport data

The kinetics of transport and inactivation dose–response data were analyzed as described previously [22]. Since cross-contaminating canalicular membrane fraction comprises an estimated $\leq 10\%$ of the total 'sinusoidal' membrane fraction [29], we estimated the impact of this degree of cross-contamination on the kinetics of GSH uptake in our SMV. The maximal effect of the cross-contribution of contaminating CMV to GSH uptake in the SMV fraction was assessed by correcting SMV transport activity (nmol (mg protein)$^{-1}$ 10 s^{-1}) at all concentrations of GSH for a 10% cross-contribution by CMV as indicated below:

$$\text{Corrected GSH transport}_{SMV} = \text{GSH transport}_{SMV} - 0.1 \times \text{net GSH transport}_{CMV})$$

where net GSH transport$_{SMV}$ and net GSH transport$_{CMV}$ are the net rates (after subtraction of non-specific binding at 0–4°C) of GSH uptake in SMV and CMV, respectively. The data defining the kinetics of GSH transport in CMV, used in these corrections, have been published earlier [22]. SMV used in the present study were obtained from identical livers that were also the source of the CMV used earlier [22]. The SAAM II program (version 1.0.3 for Macintosh) was used to perform non-linear, least squares regression fits to the kinetic as well as radiation data [35].

3. Results

3.1. Enrichment, purity and functional integrity of membrane vesicles

The SMV fractions were enriched 25- to 35-fold in Na^+,K^+-ATPase and de-enriched or not enriched in intracellular organelle markers (Table 1). The SMV fractions were ~7- and ~11-fold enriched in the canalicular markers Mg^{2+}-ATPase and alkaline phosphatase, respectively (Table 1). We confirmed the morphology and size of SMV by transmission electron microscopy (not shown). Most of the plasma membranes were vesiculated, with only a small fraction remaining in the form of sheets. The sizes of SMV estimated from these micrographs were well within the range of 0.5–1.0 μm reported by Meier et al. [29].

The Na^+-dependent transport of alanine was used as a benchmark for the functional integrity and passive permeability of SMV suspended in cryoprotective buffer [34]. All SMV used in our studies exhibited at least a 2-fold initial overshoot in alanine uptake over the final equilibrium plateau (not shown). The uptake of alanine in the presence of K^+ was minimal and did not vary significantly between preparations, indicating consistently minimal passive diffusion or 'leakiness' of our SMV. Furthermore, the radiation inactivation of Na^+-alanine cotransport was spot-checked to monitor any radiation-induced changes in the passive diffusion characteristics of SMV. In two independent SMV preparations, post-irradiation Na^+-dependent transport of alanine was found to decay mono-exponentially (data not shown). The passive diffusion of alanine as estimated by its uptake in the presence of K^+ was unaltered after 6 and 36 Mrad irradiation (not shown).

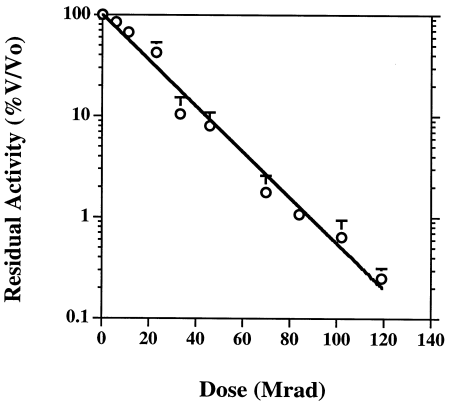

Fig. 1. Inactivation of 5′-nucleotidase. Residual activity in seven independent sinusoidal membrane vesicle preparations were pooled and the mean values are shown (circles). The solid line represents the fit of a mono-exponential function to the data weighted by S.E., represented by the bars (see functional size in text).

3.2. Inactivation of 5′-nucleotidase

In our earlier study of inactivation of GSH transport in CMV, we used the apical membrane marker 5′-nucleotidase as an internal control to monitor the dosimetry and consistency of irradiations in individual vesicle preparations [22]. An inherent attribute of the method we used to fractionate SMV is that ≤10% of the total 'sinusoidal' fraction is comprised of cross-contaminating canalicular membranes [29]. This property, evident by the presence of the apical

Table 1
Analysis of marker enzymes in sinusoidal membrane fractions[a]

Marker enzyme	Homogenate (specific activity)	Relative enrichment[c] SMV
Na^+,K^+-ATPase	15.2 ± 3.1	29 ± 7.0
Mg^{2+}-ATPase	131 ± 5.2	7.4 ± 2.2
Alkaline phosphatase	4.0 ± 0.4	11 ± 6.0
Glucose 6-phosphatase	468 ± 106	0.5 ± 0.3
Acid phosphatase	77 ± 12.1	0.5 ± 0.2
Succinic dehydrogenase	0.33 ± 0.08[b]	1.4 ± 0.6

[a]Values are mean ± S.D. of determinations in at least seven membrane preparations ($n \geq 7$). Specific activities are expressed as nmol product formed (mg protein)$^{-1}$ min^{-1}.
[b]Activity of succinic dehydrogenase is expressed as |Δabsorbance| (mg protein)$^{-1}$ min^{-1}.
[c]Relative enrichments are expressed as the ratio of specific activity in SMV to the homogenate.

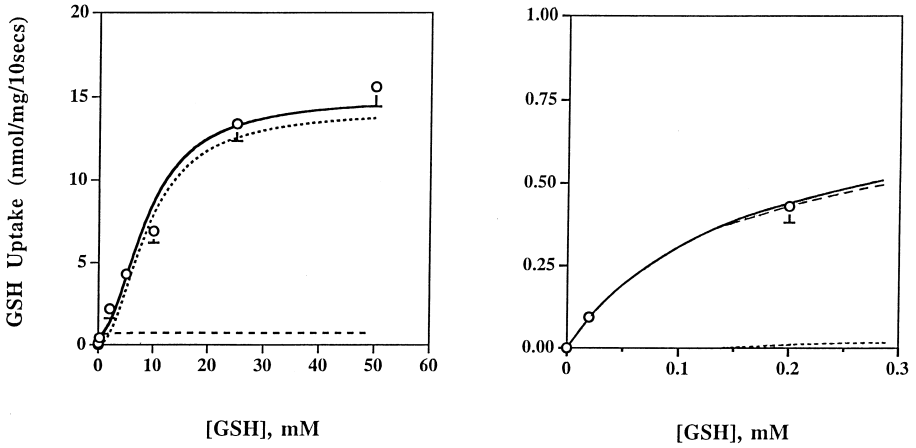

Fig. 2. Kinetics of GSH transport in non-irradiated (control) SMV. Data represent the mean ± S.D., $n = 4–7$ preparations. Initial rates of transport (10 s) were measured under voltage-clamped conditions from the uptake of [^{35}S]GSH in the presence of GSH concentrations ranging from trace (0.02 μM) to 50 mM. The continuous curve represents the overall fit to the total transport, obtained using the sum of two components, a high-affinity Michaelis–Menten unit and a low-affinity sigmoidal (Hill coefficient ~2) unit. A passive diffusion component was not required. The broken and dotted curves show the fits to the high- and low-affinity units, respectively. The right-hand panel shows the magnified version of the high-affinity region for visual appreciation of the fit and the relative contributions of the two kinetic components to the total transport. Our kinetic analysis indicated that >99.9% of transport at trace and 0.02 mM GSH is by the high-affinity component, whereas >95% of transport at 25 and 50 mM GSH is by the low-affinity component.

membrane markers Mg^{2+}-ATPase and alkaline phosphatase in our SMV (Table 1), was sufficient to allow the detection and quantification of 5′-nucleotidase in our SMV by the method we have used before [22,26]. However, as indicated below, the contribution of this degree of cross-contamination of SMV by canalicular membrane fractions had a negligible impact on the kinetics of GSH transport measured in SMV. The mean residual 5′-nucleotidase activities pooled from seven independent preparations are shown in Fig. 1, along with the mono-exponential function obtained by fitting the data. This analysis yielded a target size of 93 ± 2 kDa (mean ± S.E.). The estimated size is identical to that reported in our earlier work [22][1] and is in good agreement with the known structure of 5′-nucleotidase from past observations [32].

[1] The size of 5′-nucleotidase estimated from inactivation of this enzyme in CMV was erroneously reported as 83 ± 2 kDa in our earlier study [22]. This value should have been 93 ± 2 kDa. The correct value has subsequently been reported in a Corrigenda in Am. J. Physiol. 275 (1998) U20.

3.3. Kinetics of GSH transport in non-irradiated (control) SMV

The kinetics of GSH transport in SMV suspended in the cryoprotective buffer was indistinguishable from that in standard suspension buffers (unpublished observations). The initial rates of GSH uptake under voltage-clamped and non-voltage-clamped conditions were identical (not shown). The data representing the kinetics of GSH transport in SMV are shown in Fig. 2. Our modeling indicated that these data were consistent with and could be fitted adequately with the inclusion of only two saturable kinetic components, with no requirement for inclusion of a linear term representing passive diffusion or other non-specific effects. Our fits resolved a high-affinity unit with $K_m = 0.13 \pm 0.04$ mM, characterized by Michaelis–Menten kinetics, and a low-affinity unit with $K_m = 8.9 \pm 0.6$ mM, characterized by sigmoidal kinetics (Hill coefficient $n \sim 2$). The fit to the kinetic data, which yielded the parameter estimates indicated above, is shown in Fig. 2. The high-affinity range is expanded in Fig. 2B to assist the visual inspection of the data and the fit, as well as appreciation of the relative contributions by the high- and low-affinity components. The K_m values for both the high- and

low-affinity units estimated from our data were in the range of those published heretofore using a variety of experimental models [1,10–14]. However, there was a major distinction, in that the kinetics of transport by the low-affinity unit in our SMV uncovered the sigmoidicity that has consistently been observed in the isolated–perfused liver and isolated hepatocyte models [1,6,7,10–12], but had been absent in the SMV model [13,14]. Thus, our present observations of the low-affinity unit of GSH transport in SMV are consistent with the other more physiological models. Analysis of our kinetic data indicated that the high-affinity component has a low capacity for GSH, relative to the low-affinity unit (V_{max} ratio $\sim$5%). However, at GSH levels below 0.2 mM, the high-affinity unit mediates >99.9% of total transport while it accounts for no more than $\sim$5% of total transport at GSH levels above 25 mM. As before [22], these properties enabled us to effectively isolate the high- and low-affinity components to study their characteristics by inactivation of transport at two extremes of GSH concentration ranges, i.e., 0.02 μM (trace) and 0.02 mM vs. 25 mM and 50 mM GSH (see below).

It may be noted that a high-affinity component of GSH transport, with characteristics similar to that in SMV, has been reported in CMV [22,36,37]. Is it possible that this high-affinity component, observed in our SMV, was due to the cross-contribution from contaminating CMV? We estimated the impact of this contribution by correcting for a maximal cross-contamination (i.e., 10% of total SMV assumed to be of CMV origin) as described in Section 2. Since specific activities of GSH transport (nmol (mg protein)$^{-1}$ 10 s^{-1}) were very similar in SMV and CMV, this correction had a negligible effect on the SMV data and estimates of kinetic parameters obtained with and without correction for cross-contamination were indistinguishable.

3.4. Radiation inactivation of sinusoidal GSH transport

The high- and low-affinity components of GSH transport in SMV were studied by inactivation of GSH transport at two extremes of the GSH concentration range, i.e., at 0.02 μM (trace) and 0.02 mM vs. 25 and 50 mM GSH, as stated above.

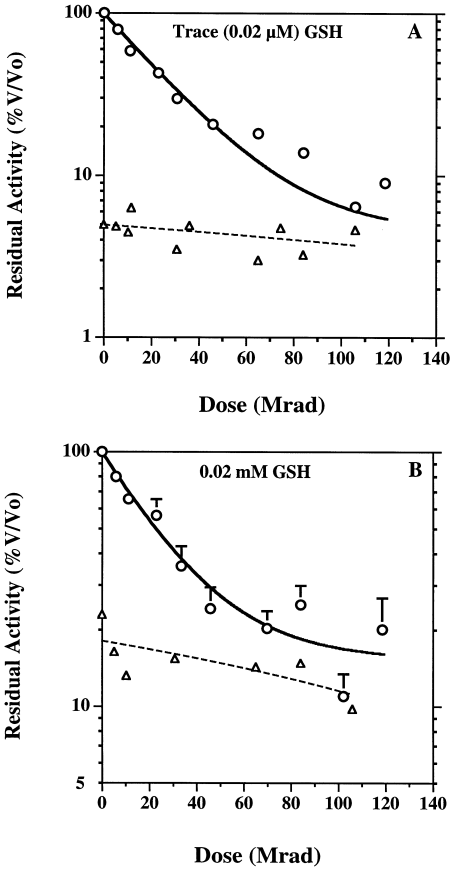

Fig. 3. Inactivation of the high-affinity transport of GSH. The mean residual transports are shown in open circles at trace GSH (A) in four independent preparations ($n=5$) and at 0.02 mM GSH (B) in seven independent preparations ($n=7$). Open triangles represent the inhibited residual GSH transport in the presence of 5 mM BSP-SG (mean of $n=2$ independent SMV preparations). The solid lines indicate the fits obtained with a mono-exponential function plus a constant equal to 5% for trace and 15% for 0.02 mM GSH. Bars represent S.E. (see estimated target sizes in text; Table 2).

3.4.1. Inactivation of the high-affinity unit

Post-irradiation transport of 0.02 μM and 0.02 mM GSH appeared to decay mono-exponentially to plateau values equivalent to $\sim$7% and $\sim$15% of their respective non-irradiated controls (Fig. 3A,B). Thus, a single exponential function without the inclusion of a radiation-insensitive component was not adequate to fit the data. The inclusion of a radiation-insensitive component was mathematically justifiable from our inactivation data, and has been used in target size analyses [33]. Nevertheless, we set out to establish an experimental basis for inclusion of such a component in our analysis by measuring the

fraction of post-irradiation transport that was truly non-inhibitable. Radiation-insensitive components may be due to 'non-specific' factors, such as binding and/or passive diffusion. Since BSP-SG is a competitive inhibitor of sinusoidal GSH transport [10], we determined the inactivation of the high-affinity component in the presence of 5 mM BSP-SG. In two independent preparations, BSP-SG was found to inhibit an average of ~95% and ~85% of transport at trace and 0.02 mM GSH, respectively, over the range of all radiation doses (Fig. 3A,B, triangles). Thus, ~5% and ~15% of unirradiated transport at trace and 0.02 mM GSH, respectively, were found to be uninhibitable, in all likelihood due to non-specific binding or passive diffusion of GSH.

On the basis of these findings, we analyzed residual transport data at 0.02 μM and 0.02 mM GSH with a single exponential plus a constant, set at 5% for 0.02 μM and 15% for 0.02 mM GSH. The fits to the data from each individual preparation resulted in the estimated target sizes listed in Table 2. The estimated mean functional sizes were 70.6 ± 4.9 kDa and 70.5 ± 6.8 kDa (mean ± S.E.) at 0.02 μM and 0.02 mM GSH, respectively. The fits to the pooled data sets are represented by the continuous lines in Fig. 3A,B. Conversely, we analyzed residual transport data by subtracting the 5% and 15% non-inhibitable fractions of transport, at 0.02 μM and 0.02 mM GSH respectively, from the initial uptake rates. The resulting functional sizes were similar to those listed in Table 2.

Table 2
Functional size[a] (kDa) of sinusoidal high-affinity GSH transporter

Preparation no.	Trace GSH; NIF = 5%	0.02 mM GSH; NIF = 15%
1	67.4	58.1
2	80.7	89.1
3	62.5	51.3
4	60.9	86.0
5	81.3	69.5
6	–	61.3
7	–	78.3
Mean ± S.E.	70.6 ± 4.9	70.5 ± 6.8

[a]Functional sizes were estimated by fitting a mono-exponential function plus a constant equal to NIF, the non-inhibitable fraction (= 5% at trace or 0.02 μM GSH and = 15% at 0.02 mM GSH) to residual transport data in five (trace GSH) and seven (0.02 mM GSH) independent preparations. NIF was estimated by inhibition of the residual transport at trace and 0.02 mM GSH by 5 mM BSP-SG (see Section 3).

3.4.2. Inactivation of the low-affinity unit

Our attempts to study the inactivation of GSH transport by the low-affinity unit in SMV, by measuring uptakes at 25 mM and 50 mM GSH, indicated that GSH transport was neither inactivated in the same manner nor to the same degree as in CMV [22]. In contrast with the radiation effects on GSH transport in CMV, there was no marked initial activation at lower doses and the overall inactivation was much less pronounced. Moreover, the smaller effects of radiation in SMV were accompanied by a relatively greater scatter in the data. Fig. 4 presents inactivation of transport for experiments conducted with 25 mM GSH. Both individual experiments as well as pooled data (inset) are shown. The data from experiments conducted with 50 mM GSH (not shown) exhibited similar characteristics, but even higher scatter, and there was no overall improvement when the data from both 25 and 50 mM GSH were pooled.

Although the pooled data shown in the inset in Fig. 4 could be fitted at face value using certain assumptions, there are serious concerns that would preclude treating the results from such analyses as reliable and representative of the actual value of the size of the transporter(s) involved. To begin with, the relatively significant activity persisting at the highest end of radiation doses (~40%) could again be in large part due to 'non-specific' factors, such as binding of GSH to small unrelated protein(s) or passive diffusion, which would not decay with irradiation. In case of the high-affinity transport of GSH in SMV, we were able to identify and correct for such 'non-specific' fractions by estimating the fraction of transport that was not inhibitable by BSP-SG. Unfortunately, it was not possible to identify and experimentally measure an analogous non-inhibitable fraction in the low-affinity transport of GSH in SMV, since a potent and specific, competitive or non-competitive inhibitor that would accomplish this aim is not known. The use of BSP-SG, a competitive inhibitor, is not feasible since the inhibition of uptake at 25 mM or 50 mM GSH would require exceedingly and prohibitively high levels of

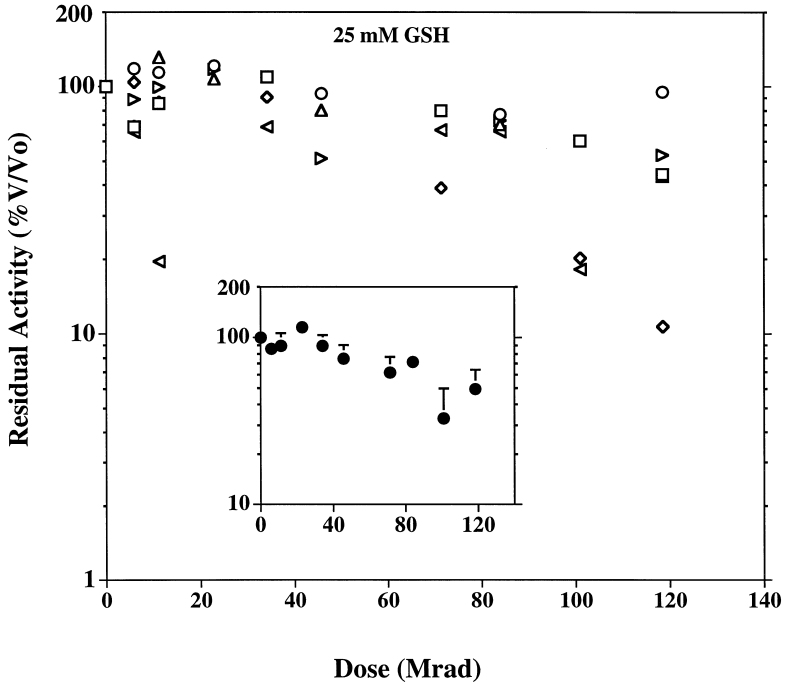

Fig. 4. Inactivation of the low-affinity transport of GSH. Inactivation of the uptake of 25 mM GSH in SMV is shown for $n=6$ individual preparations, each shown by different symbols. The lack of marked decline by irradiation, combined with considerable scatter in the data, precluded a meaningful analysis and the choice of an appropriate model to fit the data. The inset presents the means (filled circles) and S.E. (bars) of the pooled data. Some fitting attempts to the pooled data set, based on various assumptions, are described in text.

BSP-SG. Instead, we resorted to verify whether the sizable residual transport of GSH at the highest end of radiation doses would manifest *trans*-stimulation, a benchmark of carrier-mediated transport. *trans*-Stimulation of transport would rule out the possibility that all of the apparent radiation-insensitive residual activities were due to 'non-specific' effects. To that end, we spot-checked the *trans*-stimulation of the uptake of GSH by SMV, using duplicate determinations in one preparation. Transport of GSH (2 mM) into SMV that were pre-loaded with 10 mM GSH was *trans*-stimulated at all radiation doses (Fig. 5), indicating the presence of low-affinity carrier-mediated transport at higher radiation doses. Thus, it appears that a significant but unquantifiable magnitude of transport by the low-affinity unit remains at higher radiation doses, representing carrier-mediated transport rather than 'non-specific' effects.

Notwithstanding the caveats above, one could still attempt to fit the pooled data presented in the inset to Fig. 4 to gain as much insight into the range of feasible sizes for the low-affinity transporter as is possible from our data. Such analysis (not shown) resulted in a range of 12–25 kDa as the minimal estimates of the low-affinity component, obtained with mono- and bi-exponential fits without the inclusion of any radiation-insensitive component. If a pu-

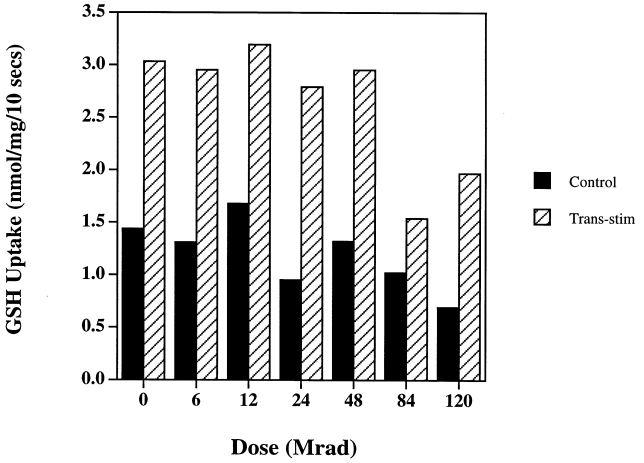

Fig. 5. *trans*-Stimulation of the uptake of 2 mM [^{35}S]GSH in sinusoidal membrane vesicles pre-loaded with 10 mM GSH. The bars represent the mean values of duplicate determinations in one preparation. As in all other cases, transport was measured under voltage-clamped conditions.

tative radiation-insensitive fraction was included, it tended to converge to ~35% of unirradiated control, yielding an estimate of ≤50 kDa for the low-affinity transporter. Potentially, this size represents the maximal estimate from our data since, in the above analysis, essentially all of the residual activities at the highest doses were treated as 'non-specific' effects. However, *trans*-stimulation of uptake counters this view, indicating that the true size of the low-affinity unit is in all likelihood lower than 50 kDa. We emphasize that given the quantity and quality of our data and the absence of any feasible methods (lack of specific inhibitor) to accurately assess the radiation-insensitive component, it is not possible to determine which of the above models is appropriate to fit the data to obtain reliable estimates. Nevertheless, regardless of the choice of model, the target size of the low-affinity sinusoidal GSH transporter appears to be smaller than the canalicular low-affinity transporter and the high-affinity system of either domain.

4. Discussion

We have succeeded in preparing SMV fractions that integrate all of the kinetic properties of GSH transport observed with different experimental models in the past into a consistent, well-behaved model. Our preparations exhibited both the high- and low-affinity components of GSH transport. However, the significant new finding was the manifestation of the sigmoidicity in the kinetics of the low-affinity component of GSH transport in SMV, which had heretofore been missing in all past studies. This attribute rendered our SMV preparations consistent with the more physiological models, such as isolated perfused livers and isolated hepatocytes. Moreover, the newly determined kinetic characteristics and parameter values, indicated negligible cross-contributions to total GSH transport by the two components at the extremes of low and high GSH concentrations, allowing us to study properties of each, individually, by target size analysis, using radiation inactivation.

The functional size of the high-affinity sinusoidal GSH transporter was resolved reliably and with precision from our inactivation data. However, unlike the canalicular low-affinity GSH transporter [22], sinusoidal low-affinity transporter was found to be much less sensitive to radiation, indicative of a considerably smaller functional unit than the low-affinity canalicular transporter. Given the quantity and quality of the inactivation data, the functional size of the low-affinity sinusoidal GSH transporter could not be estimated accurately, nor with precision. Therefore, the identification of the structural basis for multiple affinities and apparent allosterism (sigmoidicity) in the low-affinity transport of sinusoidal GSH could not be addressed meaningfully. The sigmoidal kinetics of the low-affinity transport implies positive cooperativity, either between multiple subunits in an oligomeric carrier or between multiple sites on a single polypeptide. Thus, the inability to reliably estimate the true size of the low-affinity transporter precludes any assessments as to whether the complexity in the low-affinity pathway is mediated by a single polypeptide, or an oligomer, although a very small target size does not seem plausible for an oligomer[2].

Target-size analysis of the high-affinity GSH transport in SMV indicated that it is mediated by a single protein structure, with a functional size of ~70 kDa, which is similar to that of the high-affinity component for hepatic canalicular GSH transport we have reported earlier [22]. The exact role of the high-affinity component of sinusoidal GSH transport is un-

[2] The following are other possibilities, although less likely, that could explain the modest inactivation of sinusoidal low-affinity transport. (a) We previously observed a substantial activation of the low-affinity transport of GSH in CMV at low doses (<36 Mrad) of radiation [22]. Since ~10% of the SMV used in our study may be comprised of cross-contaminating canalicular fractions, the radiation-induced activation of uptake in the contaminating CMV fractions could contribute to higher residual transport in SMV. Again, correcting the residual transport in SMV for contribution by cross-contaminating CMV did not have a significant impact on the inactivation data. (b) The sinusoidal low-affinity transport polypeptide may be less 'sensitive' to destruction by a single electron hit, requiring multiple hits for equivalent inactivation (higher radiation doses). The concept of multiple hits was postulated as an exception to target theory [38,39], but has not been experimentally established. These reports have proposed the use of a theoretical 'sensitivity' factor in target analysis to account for the putative differential susceptibility of some proteins to high-energy radiation-induced damage. Although such proteins have never been identified, in principle, their inactivation will require greater radiation exposures, relative to proteins of similar size with higher 'sensitivity'.

known, since it accounts for only a minor fraction of the total transport (it has a much lower V_{max} than the low-affinity component) and remains saturated well below the physiological levels of cellular GSH. It may be possible that the high-affinity unit transports multiple substrates. Recent studies suggest that oatp1, with unknown affinity, may function as an exchange transporter for GSH [21]. The molecular size of oatp1 ($\sim$75 kDa) happens to be quite similar to our estimate of the high-affinity sinusoidal GSH transporter. On the other hand, a number of physiological features of sinusoidal GSH transport, which have been observed at the low-affinity ranges of GSH transport, such as response to membrane potential and thiol-disulfides, e.g., cystine and DTT [6,7], strongly indicate that oatp1 cannot be the major and primary low-affinity sinusoidal GSH transporter, accounting for the bulk of physiological GSH efflux.

The functional size of the high-affinity GSH carrier in SMV is also similar to that of the high-affinity GSH carrier in CMV [22]. Taking into consideration that the two proteins share common functions and features in catalyzing the transport of GSH, it is possible that the high-affinity uptake of GSH in SMV and CMV are mediated by the same protein or by proteins that belong to the same family.

In conclusion, our studies clearly reveal that the high- and low-affinity components of hepatic sinusoidal transport of GSH are mediated by distinct carriers with dissimilar susceptibility to inactivation by irradiation. The low-affinity sinusoidal transporter of GSH is smaller than the canalicular low-affinity transporter and the high-affinity transporters of either basolateral or apical plasma membrane domains. The high-affinity sinusoidal transporter of GSH exhibits a functional size similar to both oatp1 and the canalicular high-affinity GSH transporter.

Acknowledgements

This study was supported by National Institutes of Health Grants R01 AG-07467 and R37 DK-30312. Rat liver membrane vesicles were prepared and provided by the Subcellular-Organelle Core and mathematical analyses and fitting of the data were conducted by the Kinetic and Mathematical Modeling Core of USC Research Center for Liver Diseases (P30 DK-48522).

References

[1] M. Ookhtens, T. Maddatu, Mechanism of changes in hepatic sinusoidal and biliary GSH efflux with age in rats, Am. J. Physiol. 261 (1991) G648–G656.
[2] N. Kaplowitz, T.Y. Aw, M. Ookhtens, The regulation of hepatic glutathione, Annu. Rev. Pharmacol. Toxicol. 25 (1985) 715–744.
[3] A. Meister, M.E. Anderson, Glutathione, Annu. Rev. Biochem. 52 (1983) 711–760.
[4] M. Ookhtens, A.V. Mittur, Developmental changes in plasma thiol-disulfide turnover in rats: a multicompartmental approach, Am. J. Physiol. 267 (1994) R415–R425.
[5] M. Ookhtens, N. Kaplowitz, Role of the liver in interorgan homeostasis of glutathione and cyst(e)ine, Semin. Liver Dis. 18 (1998) 313–329.
[6] S.C. Lu, J. Ge, H. Huang, J. Kuhlenkamp, N. Kaplowitz, Thiol-disulfide effects on hepatic glutathione transport studies in cultured rat hepatocytes and perfused livers, J. Clin. Invest. 92 (1993) 1188–1197.
[7] S.C. Lu, J. Kuhlenkamp, J. Ge, W. Sun, N. Kaplowitz, Specificity and directionality of thiol effects on sinusoidal glutathione transport in rat liver, Mol. Pharmacol. 46 (1994) 578–585.
[8] C.K. Sen, L. Packer, Antioxidant and redox regulation of gene-transcription, FASEB J. 10 (1996) 709–720.
[9] P.S. Samiec, C. Drews-Botsch, E.W. Flagg, J.C. Kurtz, P. Sternberg Jr., R.L. Reed, D.P. Jones, Glutathione in human plasma: Decline in association with aging, age-related macular degeneration, and diabetes, Free Radic. Biol. Med. 24 (1998) 699–704.
[10] M. Ookhtens, K. Hobdy, M.C. Corvasce, T.Y. Aw, N. Kaplowitz, Sinusoidal efflux of glutathione in the perfused rat liver. Evidence for a carrier-mediated process, J. Clin. Invest. 75 (1985) 258–265.
[11] T.Y. Aw, M. Ookhtens, C. Ren, N. Kaplowitz, Kinetics of GSH efflux from isolated rat hepatocytes, Am. J. Physiol. 250 (1986) G236–G243.
[12] S.C. Lu, C. Garcia-Ruiz, J. Kuhlenkamp, M. Ookhtens, M. Salas-Prato, N. Kaplowitz, Hormonal regulation of glutathione efflux, J. Biol. Chem. 265 (1990) 16088–16095.
[13] J.C. Fernandez-Checa, M. Ookhtens, N. Kaplowitz, Selective induction by phenobarbital of the electrogenic transport of glutathione and organic anions in rat liver canalicular membrane vesicles, J. Biol. Chem. 268 (1993) 10836–10841.
[14] M.R. Inoue, R. Kinne, T. Tran, I.M. Arias, Glutathione transport across hepatocyte plasma membranes. Analysis using isolated rat-liver sinusoidal-membrane vesicles, Eur. J. Biochem. 138 (1984) 491–495.
[15] T.Y. Aw, M. Ookhtens, N. Kaplowitz, Inhibition of gluta-

thione efflux from isolated rat hepatocytes by methionine, J. Biol. Chem. 259 (1984) 9355–9358.
[16] J.C. Fernandez-Checa, C. Garcia-Ruiz, A. Colell, J.R. Yi, N. Kaplowitz, Inhibition of rat sinusoidal GSH transporter by thioethers-specificity, sidedness, and kinetics, Am. J. Physiol. 33 (1996) G969–G975.
[17] N. Kaplowitz, J. Fernandez-Checa, M. Ookhtens, Hepatic glutathione transport, in: N. Taniguchi, T. Higashi, Y. Sakamoto, A. Meister (Eds.), Glutathione Centennial: Molecular Perspectives and Clinical Implications, Academic Press, San Diego, CA, 1990, pp. 395–406.
[18] M. Ookhtens, I. Lyon, J.C. Fernandez-Checa, N. Kaplowitz, Inhibition of GSH efflux in the perfused rat liver and isolated hepatocytes by organic anions and bilirubin: kinetics, sidedness, and molecular forms, J. Clin. Invest. 82 (1988) 608–616.
[19] C. Garcia-Ruiz, J.C. Fernandez-Checa, M. Ookhtens, N. Kaplowitz, Bidirectional mechanism of plasma-membrane transport of reduced glutathione in intact rat hepatocytes and membrane-vesicles, J. Biol. Chem. 267 (1992) 22256–22264.
[20] J. Yi, S. Lu, J.C. Fernandez-Checa, N. Kaplowitz, Expression cloning of the cDNA for a polypeptide associated with rat hepatic sinusoidal reduced GSH transport: characteristics and comparison with the canalicular transporter, Proc. Natl. Acad. Sci. USA 92 (1995) 1495–1499.
[21] L.Q. Li, T.K. Lee, P.J. Meier, N. Ballatori, Identification of glutathione as a driving-force and leukotriene C-4 as a substrate for oatp1, the hepatic sinusoidal organic solute transporter, J. Biol. Chem. 273 (1998) 16184–16191.
[22] A.V. Mittur, N. Kaplowitz, E.S. Kempner, M. Ookhtens, Novel properties of hepatic canalicular reduced glutathione transport revealed by radiation inactivation, Am. J. Physiol. 37 (1998) G923–G930.
[23] E.S. Kempner, Novel predictions from radiation target analysis, Trends Biol. Sci. 18 (1993) 236–239.
[24] E.S. Kempner, Damage to proteins due to the direct action of ionizing radiation, Q. Rev. Biophys. 26 (1993) 27–49.
[25] M.W. Fariss, D.J. Reed, High-performance liquid chromatography of thiols and disulfides: dinitrophenol derivatives, Methods Enzymol. 143 (1987) 101–109.
[26] A. Amici, M. Emanuelli, N. Raffaelli, S. Ruggieri, G. Magni, One-minute high-performance liquid chromatography assay for 5′-nucleotidase using a 20-mm reverse-phase column, Anal. Biochem. 216 (1994) 171–175.
[27] G. Whelan, J. Hoch, B. Combes, A direct assessment of the importance of conjugation for biliary transport of sulfobromopthalein sodium, J. Lab. Clin. Med. 75 (1970) 542–557.
[28] C.A. Snel, Y. Zhao, G.J. Mulder, K.S. Pang, Methods for the quantitation of bromosulfophthalein and its glutathione conjugate in biological fluids, Anal. Biochem. 212 (1993) 28–34.
[29] P.J. Meier, E.S. Sztul, A. Reuben, J.L. Boyer, Structural and functional polarity of canalicular and basolateral plasma membrane vesicles isolated in high yield from rat liver, J. Cell Biol. 98 (1984) 991–1000.
[30] J.C. Fernandez-Checa, H. Takikawa, T. Horie, M. Ookhtens, N. Kaplowitz, Canalicular transport of reduced glutathione in normal and mutant Eisai hyperbilirubinemic rats, J. Biol. Chem. 267 (1992) 1667–1673.
[31] J.T. Harmon, T.B. Nielsen, E.S. Kempner, Molecular weight determinations from radiation inactivation, Methods Enzymol. 117 (1985) 65–94.
[32] E.S. Kempner, Molecular size determination of enzymes by radiation inactivation Adv, Enzymol. Relat. Areas Mol. Biol. 61 (1988) 107–147.
[33] E.S. Kempner, The mathematics of radiation target analyses, Bull. Math. Biol. 57 (1995) 883–898.
[34] P.J. Meier, A.S. Meier-Abt, C. Barrett, J.L. Boyer, Mechanisms of taurocholate transport in canalicular and basolateral rat liver plasma membrane vesicles. Evidence for an electrogenic canalicular organic anion carrier, J. Biol. Chem. 259 (1984) 10614–10622.
[35] SAAM II User's Guide. SAAM Institute, University of Washington, Seattle, WA, 1994.
[36] N. Ballatori, W.J. Dutczak, Identification and characterization of high and low affinity transport systems for reduced glutathione in liver cell canalicular membranes, J. Biol. Chem. 269 (1994) 19731–19737.
[37] S.C. Lu, J. Kuhlenkamp, H. Wu, W. Sun, L. Stone, N. Kaplowitz, Progressive defect in biliary GSH secretion in streptozotocin-induced diabetic rats, Am. J. Physiol. 272 (1997) G374–G382.
[38] A.S. Verkman, K. Skorecki, D.A. Ausiello, Radiation inactivation of oligomeric enzyme systems: theoretical considerations, Proc. Natl. Acad. Sci. USA 81 (1984) 150–154.
[39] S. Swillens, Inactivation of macromolecules by ionizing radiation. Deterministic single-hit or stochastic multievent process?, Biochem. J. 233 (1986) 655–659.